CONTEXT-BASED TEMPLATE MATCHING IN IRIS RECOGNITION

C. Rathgeb and A. Uhl

Department of Computer Sciences
University of Salzburg, A-5020 Salzburg, Austria

ABSTRACT

In general iris recognition algorithms restrict to extracting distinct features out of preprocessed iris images in order to create user-specific iris-codes, neglecting potential improvements in matching procedures. In this work we propose a new way of matching iris-codes. By exploiting local information of extracted iris-codes a context-based matching is performed. The matching procedure is applied to a trivial iris-code generation as well as existing iris recognition systems. Experimental results, according to recognition rates as well as time measurements, emphasize the worthiness of our approach.

***Index Terms*—** Biometrics, Iris Recognition, Context-based Matching

1. INTRODUCTION

In order to overcome the protection of crucial information through weak passwords or PINs a tremendous interest in biometrics has emerged. Over the past years several biometric modalities have been established suitable to be used for personal identification [1], whereas the iris is one of the most reliable [2]. Depending on the iris recognition system the matching process is performed according to a specified metric. Altough several metrices exist most iris recognition systems resort to applying simple metrices, such as the normalized Hamming distance, in order to provide a fast matching process. However, these simple metrices do not necessarily show the best results, according to the applied algorithm.

Besides breakthrough work regarding iris recognition, proposed by Daugman [3] and Wildes [4] several approaches have been presented suggesting many different filters to be used in the feature extraction step (see [2]). Most of these approaches show practical performance on diverse test sets, reporting recognition rates above 99% and equal error rates of less than 1%. Yet most of these algorithms restrict to applying simple metrices in the matching process, such as the Hamming distance. To our knowledge Ring and Bowyer [5] were the only one to examine the structure of binary iris codes. The authors attempt to detect distortions of iris texture through analyzing iris code matching results. In this work

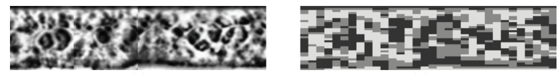

(a) (b)

Fig. 1. Discretization: (a) preprocessed texture (b) discretized texture using four different codewords and blocks of 8×2 pixel (each grayscale block represents a codeword).

we present a new approach to matching iris-codes which we refer to as *context-based matching*. Intuitively, large connected matching parts of iris-codes indicate genuine samples. On the other hand, large connected non-matching areas as well as rather small matching areas of iris-codes indicate non-genuine samples tending to cause more randomized distortions. Based on these logically justifiable assumptions iris-codes are analyzed.

This paper is organized as follows: first the proposed is described in detail, based on a trivial feature extraction (Sect. 2). Subsequently, experimental results are presented, discussed and the proposed matching procedure is applied to other iris recognition algorithms (Sect. 3). Finally a conclusion is given (Sect. 4).

2. ALGORITHM

We put the main focus on the matching procedure, comparing iris-codes extracted from preprocessed iris images. In order to describe the matching procedure a rather simple feature extraction is introduced.

Preprocessing is adjusted to Daugman's approach [3]. After approximating the inner and outer boundary of the iris, the resulting iris ring is unwrapped in order to generate a normalized rectangular texture. Due to the fact that the top and bottom of the iris are often hidden by eyelashes or eyelids, these parts of the iris are discarded (315^o to 45^o and 135^o to 225^o). To obtain a smooth image a Gaussian blur is applied to the resulting iris texture. To enhance the contrast we use an advanced contrast enhancement technique called CLAHE [6]. This algorithm operates on local image regions where the image is subdivided into image tiles and the contrast is enhanced within each of these regions. A preprocessed iris texture is illustrated in Fig. 1 (a). In the feature extraction blocks of $x \times y$ pixels of preprocessed iris textures are examined and each block is discretized by mapping the grayscale

This work has been supported by the Austrian Science Fund, project no. L554-N15.

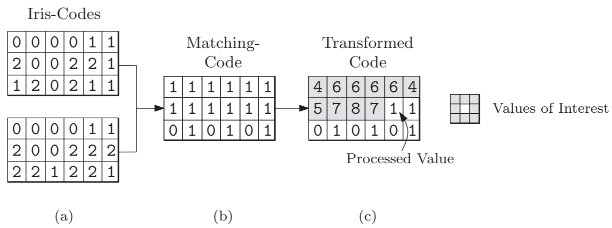

Fig. 2. The Matching Process: (a) two sample parts of iris-codes composed of three different codewords (b) the binary matching-code resulting out of these iris-codes (c) the transformed matching-code for the defined values of interest.

values of all included pixels p_i to a natural number less than a predefined parameter k such that,

$$p_i \mapsto \left\lfloor \frac{p_i}{\frac{n}{k}} \right\rfloor \tag{1}$$

where n is the number of possible grayscale values. Subsequently, the most frequent value of each block is assigned to the entire block, defining the codeword of the block. The process of discretization is shown in Fig. 1. Two-dimensional iris-codes, with respect to the resulting number of rows, are generated by concatenating the resulting codewords of all discretized $x \times y$ blocks. Example parts of tertiary iris-codes ($k = 3$) are illustrated in Fig. 2 (a).

2.1. Context-based Matching

The matching process consists of two steps: firstly, a so-called *matching-code* is generated out of two iris-codes to be matched. In the second step values the matching-code are transformed and a final *matching score* is calculated.

The matching-code is generated by laying one iris-code on top of another, where codewords of both iris-codes are compared and 1s are assigned to matching codewords and 0s to non-matching codewords. Iris-codes need not necessarily be two-dimensional, however, within most iris recognition algorithms, distinct parts of iris-codes originate from distinct parts of proprocessed textures. Thus, most iris-codes can be adjusted in rows to generate two-dimensional matching-codes providing more local information. In Fig. 2 (a)-(b) this process is shown for parts of two sample iris-codes.

In the next step the two-dimensional matching-code, consisting of 1s and 0s, is examined, in order to find connected areas of matching as well as non-matching codewords (clusters of 1s and 0s). That is, for each value of the matching-code, predefined neighboring values of interest are considered (these need not be identical). In Fig. 3 several examples of neighboring values of interest for matching and non-matching codewords (1s and 0s in the matching-code) are shown. The initial values of the two-dimensional matching-code are then transformed to decimal values dependent on their neighboring values of interest, as shown in Fig. 2 (c). If a processed value of the matching code is 1 it is incremented for each value of interest which is 1 as well. By analogy, if a processed value

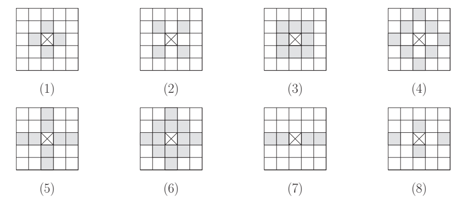

Fig. 3. Values of Interest: several different meaningful combinations of values of interest (filled gray), where the centered cell represent a processed value of a matching-code.

is 0 it is decremented for each value of interest which is 0. By definition, our algorithm only increments a value of the matching-code resulting from matching codewords, while it only decrements a value of the matching-code resulting from non-matching codewords (1s and 0s respectively). Fig. 2 (c) shows an example of this process, where the transformation is applied to each value of a matching-code. We calculate the matching-score of two iris-codes IC_i and IC_j, denoted by $M_{IC_i IC_j}$, which declares the grade of similarity of these iris-codes, by summing up the signed powers of two of all values v_l of the matching-code such that,

$$M_{IC_i IC_j} = \sum_{l=1}^{N} \mathrm{sgn}(v_l) \cdot 2^{|v_l|} \tag{2}$$

where N denotes the total number of values of the matching-code and $\mathrm{sgn}(x)$ the signum function, respectively. Thereby large connected clusters become highly valuable. The larger the matching score the higher the grade of similarity. Minimum and maximum matching-scores depend on the predefined values of interest for matching as well as non-matching codewords and the dimension of the matching code. An adequate threshold, which can be found by testing a certain set of iris images, for the calculated matching-score yields a successful authentication or rejection, respectively.

3. EXPERIMENTS

Experiments are performed using the CASIAv3-Interval [7] iris database. In the preprocessing step 512×64 pixels iris textures are extracted (slitted iris textures are of size 256×64 pixels). First we apply the above presented iris-code generation. Subsequently, the matching procedure is adapted to our own implementations of existing iris recognition algorithms which show good performance using the Hamming distance as metric. Since context-based matching is more complex than simple metrices, finally time measurements are presented and discussed. All applied algorithms are implemented in C and tested on a 1.3 GHz Linux system.

3.1. Proposed Algorithm

For the proposed iris-code generation several parameters have to be set up: dimension of pixel blocks, number of different codewords assigned to these blocks and values of interest

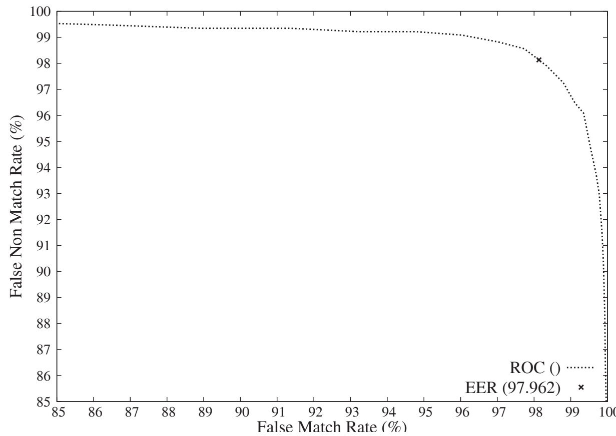

Fig. 4. ROC of the proposed algorithm using 8×2 blocks, three grayscale values and Hamming distance as metric.

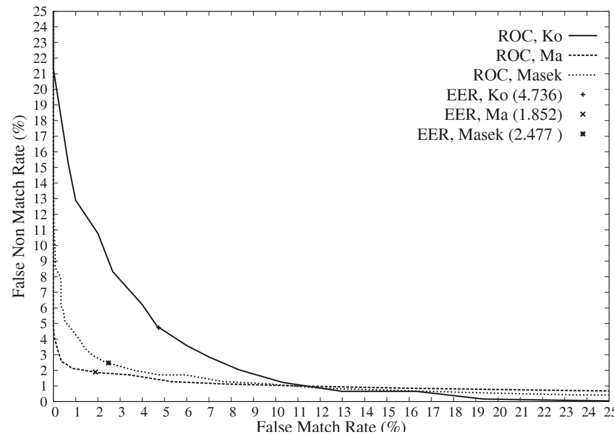

Fig. 5. ROC of the algorithm of Ko using lower Hamming distance as metric and Ma and Masek using Hamming distance as metric.

for matching and non-matching codewords. In all experiments best rates were achieved using 8×2 pixel blocks. Additionally, in all experiments a circular shift of the preprocessed texture (5 pixels to the left and right) is performed to provide rotation-invariance. Processed values resulting from matching codewords are further increased if a matching value of interest results from a different codeword. Thereby, matching parts of the iris-code originating from transitions of grayscale values become more valuable. Processed values resulting from non-matching codewords are further decreased if a non-matching value of interest results from the same codeword. The receiver operating characteristic (ROC) curve using three different codewords ($k = 3$) is plotted in Fig. 6, referring to Fig. 3 values of interest (4) are applied for matching codewords and values of interest (3) are applied to non-matching codewords. For these parameters we obtained best experimental results. Since an iris texture is a natural image immediate neighboring values of interest do not contain useful information for matching codewords, these tend to be equal. On the other hand, comprehensive non-matching parts of iris-codes are tracked by examining just adjacent values. According to the values of interest (see Fig. 3) several of these have been tested. Best results applying three grayscale values are summarized in Tab. 1. In contrary the ROC curve with regard to the normalized Hamming distance of the generated iris codes, using three different grayscale values, is plotted in Fig. 4. For the presented iris-code generation applying the Hamming distance as metric does not work at all. Since multi-sample enrollment increases the performance of a biometric recognition system [8, 9] we applied the same algorithm using several enrollment samples where the maximum match-score of these is returned. Using the same parameters recognition rates are summarized in Tab. 1.

3.2. Alternative Algorithms

Additionally, we applied the proposed matching procedure to our implementations of the iris recognition algorithms of Ko *et al.* [10], Ma *et al.* [11] and Masek [12]. The algorithm

Table 1. Performance Measurements for the prop. Algorithm

VoI Match	VoI Non-Match	FNMR at 0% FMR	En. Sam.
(1)	(1)	5.61	1
(2)	(2)	3.34	1
(3)	(3)	2.98	1
(4)	(3)	2.24	1
(5)	(3)	7.08	1
(6)	(3)	6.71	1
(4)	(3)	1.36	2
(4)	(3)	0.95	3

of Ko uses cumulative sum based change analysis to analyze preprocessed iris textures. Iris textures are divided into cells out of which mean gray scale values are calculated and furthermore, upward and downward slopes of grayscale values are detected, according to appropriate groups. For the suggested parameters, a cell dimension of 10×3 pixels is used and horizontal and vertical groups of five cells iris-codes consisting of 50×40 bits are extracted. In the matching process the lower Hamming distance is used as metric where differences in up- and downward slopes are counted. In the algorithms of Ma and Masek the upper 512×50 pixel of the preprocessed iris textures are examined and mean values of blocks of 1×5 pixel are processed. In the algorithm of Ma a 1-D wavelet transform is applied to ten 1-D intensity signals of length 512. Detected minima and maxima serve as features where sequences of 1s and 0s are assigned to the iris-code until new maxima or minima are found. This whole process is applied to two subbands extracting a total number of $2 \times 512 \times 10 = 10240$ bits. As well as Ma, Masek analyzes ten 1-D intensity signals where complex values in the transform-domain of the Log-Gabor transformation are encoded with 2 bits per 1×5 pixel block extracting an iris-code of $512 \times 10 \times 2 = 10240$ bits. The generated iris-codes of both algorithms are arranged in a two-dimensional manner. The algorithm of Ma extracts a 512×20 bit iris-code, 512×10 bits for both subbands, and the algorithm of Masek extracts

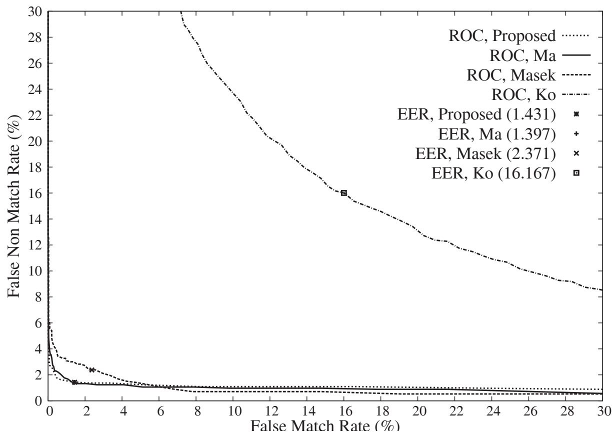

Fig. 6. ROC of the proposed algorithm using 8×2 blocks, 3 grayscale values, (4) for matching and (3) for non-matching codewords and the algorithm of Ko, Ma and Masek using (7) for matching and (7) for non-matching codewords.

a 1024×10 bits iris-code. The ROC curves of the algorithm of Ko, Ma and Masek are plotted in Fig. 5, revealing equal error rates (EERs) of 4.734%, 1.852% and 2.477%, where the first iris image of each person is used as enrollment sample. For all algorithms we applied context-based matching. The ROC curves for best experimental results for the algorithm of Ko , Ma and Masek are shown in Fig. 6. While EERs for the algorithm of Ma and Masek decrease by 0.455% and 0.106%, respectively, context-based matching fails for the algorithm of Ko, the EER is increased by 11.431%. In the original algorithm of Ko some sort of context-based matching is applied, counting mismatching sequences of up- and downward slopes of cumulative sums, thus, further context based matching does not pay off.

3.3. Time Measurement

Obviously, the proposed context-based matching procedure is more complex then measuring the Hamming distance between iris-codes. Speaking of identification a system has to perform one feature extraction and n tests, where n is the number of stored templates in a database. Thus, for a great number of n a simple matching process will achieve better performance, regardless to the cost of the feature extraction. In verification mode the system has to perform one feature extraction and one test (against a specific template stored for the claimed identity). In this case a comparison of the feature extraction cost and the matching cost is meaningful. Time measurements, carried out for best results, are summarized in Tab. 2. As can be seen the proposed feature extraction method is about twice as fast as those of Ma and Masek. For context-based matching all algorithms tend to require almost the same time, which depends on the number of values of interest and the size of iris-codes. If times of feature extraction and matching are summed up, as it is the case in verification mode, our algorithm is still about two times faster than those of Ma and Masek revealing comparable performance results.

Table 2. Time Measurements (sec.)

	Proposed	Ma *et al.*	Masek
Feature Extr.	0.061370	0.134562	0.108114
Context Match	0.006694	0.025955	0.025788
HD Match	–	0.013751	0.017117

4. CONCLUSION

In this work we present a new way of comparing iris-codes which we refer to as context-based matching. For the proposal of a trivial feature extraction performance results are satisfying, by all means comparable to well-established approaches. Due to the simplicity of the feature extraction the more complex matching procedure does not decelerate performance in verification mode. Furthermore, the proposed matching procedure is adapted to existing systems increasing the performance of these.

5. REFERENCES

[1] A. K. Jain, P. J. Flynn, and A. A. Ross, *Handbook of Biometrics*, Springer-Verlag, 2008.

[2] K. W. Bowyer, K. Hollingsworth, and P. J. Flynn, "Image understanding for iris biometrics: a survey," *Computer Vision and Image Understanding*, vol. 110, pp. 281–307, 2008.

[3] J. Daugman, "How Iris Recognition Works," *IEEE Trans. CSVT*, vol. 14, no. 1, pp. 21–30, 2004.

[4] R. P. Wildes, "Iris recognition, in: Biometric Systems: technology, Design and Performance Evaluation," *Springer-Verlag*, pp. 63–95, 2005.

[5] S. Ring and K.W. Bowyer, "Detection of iris texture distortions by analyzing iris code matching results," in *Biometrics: Theory, Applications and Systems (BTAS'08)*, 2008, pp. 1–6.

[6] K. Zuiderveld, *Graphics Gems IV*, chapter Contrast Limited Adaptive Histogram Equalization, pp. 474–485, Morgan Kaufmann, 1994.

[7] "The Center of Biometrics and Security Research, CASIA Iris Image Database, http://www.sinobiometrics.com," .

[8] K. W. Bowyer, K. I. Chang, P. Yan, P. J. Flynn, E. Hansley, and S. Sarkar, "Multi-modal biometrics: an overview," *Second Workshop on Multi-Modal User Authentication*, 2006.

[9] Y. Du, "Using 2D log-Gabor spatial filters for iris recognition," *SPIE 6202: Biometric Technology for Human Identification III*, pp. 62020:F1–F8, 2006.

[10] J.-G. Ko, Y.-H. Gil, and J.-H. Yoo, "Iris Recognition using Cumulative SUM based Change Analysis," *Intelligent Signal Processing and Communications, 2006. ISPACS'06*, pp. 275–278, 2006.

[11] L. Ma, T. Tan, Y. Wang, and D. Zhang, "Efficient Iris Recognition by Characterizing Key Local Variations," *IEEE Transactions on Image Processing*, vol. 13, no. 6, pp. 739–750, 2004.

[12] L. Masek, "Recognition of Human Iris Patterns for Biometric Identification, Master's thesis, University of Western Australia, 2003," .